A NOVEL MICROMACHINED LIQUID PROPERTY SENSOR UTILIZING A DOUBLY CLAMPED VIBRATING BEAM

Erwin K. Reichel[1], Bernhard Weiß[1], Christian Riesch[2], Artur Jachimowicz[2], Bernhard Jakoby[1]

[1] Institute for Microelectronics, Johannes Kepler University Linz
Altenbergerstr. 69, 4040 Linz, Austria
Phone: +43 732 2468 9301, Fax: +43 732 2468 9316
[2] Institute of Sensor and Actuator Systems, Vienna University of Technology
Gusshausstrasse 27 – 29, A-1040 Vienna, Austria

*Corresponding Author: Erwin Reichel, erwin.reichel@jku.at

Abstract – A novel miniaturized sensor for the online measurement of the mechanical properties of a viscous liquid utilizing a resonating beam has been designed and fabricated in silicon technology. The modeling of the electromagnetic actuation of the device is discussed and the response of a first prototype was experimentally characterized using impedance spectroscopy.

Keywords: Viscosity Measurement, Oscillating Beam, Online Fluid Sensor

INTRODUCTION

Micromachined vibrating structures are becoming more attractive for sensing applications due to their size and cost–effectiveness. Single–ended cantilever structures are commonly used in atomic force microscopy [1], as mass–sensitive devices [2], and biosensors [3] in both, liquid and gaseous environments. A precise modeling of the solid–liquid interaction and the measurement of the frequency response enables the measurement of the density and the rheological behaviour of liquids [4] in a way comparable to quartz–disk viscosity sensors [5], [6]. As demonstrated in [7] the usually lower resonance frequency and different flow field characteristics make the measurements more comparable to those performed with laboratory viscometers, even for liquids showing non–Newtonian behaviour [8].

In this contribution, we investigate the vibrational behaviour of an immersed doubly–clamped beam excited by the Lorentz force emerging from a sinusoidal current through the conductive path in a static magnetic field. Vibrating viscosity sensors usually measure a quantity proportional to the product of the fluid density and viscosity by analyzing the frequency shift and damping of a single mode. Utilizing normal and torsional modes, the viscosity and density values can potentially be determined seperately. For modeling the liquid–solid interface, a numerical method based on Green's functions in the spatial frequency domain was implemented for calculating the flow around a harmonically vibrating, infinitely thin plate providing the viscous damping force and added mass for each mode of interest. Based on the equivalent spring constant and damping coefficient, an electrical equivalent circuit model is derived, describing a small but measurable effect in the impedance spectrogram.

A first prototype of a vibrating viscosity sensor was manufactured in silicon technology and characterized without liquid loading.

THEORY

The fluid is described by the Navier–Stokes and the continuity equations

$$\rho_f \left(\frac{\partial \mathbf{v}}{\partial t} + (\mathbf{v} \cdot \nabla)\mathbf{v} \right) = \mathbf{f} - \nabla p + \mu \Delta \mathbf{v} + (\lambda + \mu) \nabla (\nabla \cdot \mathbf{v})$$
$$\frac{\partial \rho_\mathbf{f}}{\partial t} + \nabla \cdot (\rho_f \mathbf{v}) = 0, \qquad (1)$$

where $\mathbf{v}$, p, μ, λ, ρ_f describe flow velocity, pressure, first and second coefficient of viscosity, and density of the liquid respectively. The convective term $\rho(\mathbf{v} \cdot \nabla)\mathbf{v}$ is neglected, because its influence on the solution at small vibration amplitudes is negligible [9].

Considering the equation of motion of the vibrating beam, the interaction with the viscous fluid can be modeled by adding a viscous damping term per unit length, α, and an added mass term per unit length, m_f, to the Bernoulli–Euler beam equation (see below). The added mass term accounts for the fluid, which follows the oscillation of the beam and therefore increases the actual vibrating mass, whereas the viscous damping term considers the damping due to the induced pressure waves on both faces of the beam and the friction in the induced flow. Since the beam is doubly clamped, intrinsic stresses are present, which are considered by means of a prestress term in the beam equation [10]

$$EJ \frac{\partial^4 w}{\partial x^4} - N \frac{\partial^2 w}{\partial x^2} + (\rho_b A + m_f) \frac{\partial^2 w}{\partial t^2} + \alpha \frac{\partial w}{\partial t} = q(x,t), \qquad (2)$$

where w, N, ρ_b, EJ, A, L_b describe the deflection, the prestressing force, the mass density, the product of Young's modulus and geometrical inertia, the cross–sectional area, and the length of the beam respectively. The resulting resonance angular frequencies are given by

$$\omega_{rd,n}^2 = \frac{(\rho_b A + m_f)(EJ\kappa_n^4 + N\kappa_n^2) - \alpha^2/4}{(\rho_b A + m_f)^2}, \qquad (3)$$

where κ_n for a certain vibration mode n is obtained by the n^{th} root of the equation $\cos(\kappa_n L_b)\cosh(\kappa_n L_b) = 1$,

which can be approximated by $\kappa_n \cong (1/2+n)\pi/L_b$. The added mass and the damping coefficients are determined by computing the actual resistance of the fluid on the vibrating structure by means of $\oint_S p(s)ds$, where S is the enclosed surface of the cantilever and $p(s)$ the pressure, respectively. In [11] Tuck calculates the resistance force per unit length on a circular cylinder of the diameter B vibrating harmonically in the y-direction in incompressible fluid as (using complex notation)

$$F_{res}(t) = (k - jk')\rho\pi(B/2)^2\omega^2 U_{y,0}e^{j\omega t}, \quad (4)$$

where $U_{y,0}$ is the maximum y-deflection, and k is the ratio between added and displaced mass. The parameters k and k' depend on the Reynold's number of the flow $Re = B^2\omega\rho/4\mu$

$$k - jk' = 1 - \frac{4K_1(\sqrt{jRe})}{\sqrt{jRe}K_0(\sqrt{jRe})}, \quad (5)$$

where K_0 and K_1 are the modified Bessel functions of the second kind. From Eqn. 4 the added mass and the damping can be obtained as $m_f = -k\rho\pi(B/2)^2$ and $\alpha = -k'\omega\rho\pi(B/2)^2$.

In this work the beam shows a rectangular cross–section and is approximated by an infinitely thin plate along the x–axis vibrating in a compressible fluid (in y–direction), where the convective term is neglected. By using the adiabatic compressibility coefficient $\zeta_s = \rho^{-1}(\partial\rho/\partial p)_s$, assuming small perturbations p_e and ρ_e about their equilibrium values p_0 and ρ_0, and by introducing time–harmonic values of pressure p and displacement $\mathbf{u}$ (e. g. $\mathbf{u} = \Re\{\mathbf{u}_0 e^{j\omega t}\}$) the system

$$\nabla^2\underline{\mathbf{u}} + \gamma\nabla(\nabla\cdot\underline{\mathbf{u}}) + \beta\underline{\mathbf{u}} = 0 \quad (6)$$

$$p_e = -\zeta_s^{-1}(\nabla\cdot\mathbf{u}) \quad (7)$$

with the constants $\beta = -j\omega\rho_0/\mu$ and $\gamma = 1 + \lambda/\mu - j/(\omega\mu\zeta_s)$ arises [9]. After applying a spatial Fourier transform with respect to x, e. g.

$$\underline{u}_x(x,y) = \mathcal{F}^{-1}\{\underline{U}_x(k_x,y)\} = \int_{-\infty}^{\infty}\underline{U}_x(k_x,y)e^{-jk_x x}dk_x$$

on Eqn. 6, a linear system in the Fourier domain $\partial\underline{\mathbf{\Psi}}/\partial y = \underline{\mathbf{A}}.\underline{\mathbf{\Psi}}$ with the variables $\underline{\mathbf{\Psi}} = [\underline{U}_x, \underline{U}_y, \partial\underline{U}_x/\partial y, \partial\underline{U}_y/\partial y]^T$ results. These equations are used to expand the fields in terms of spectral eigenmodes.

Using this expansion in both halfspaces ($y^+ > 0$, $y^- < 0$) and imposing discontinuities of $\partial\underline{U}_y/\partial y$ at the interface ($y^+, y^- = 0$), the displacement field U_y due to an y–oriented surface force distribution $\underline{F}_{s,y}(x)$ at the interface can be obtained. Choosing $\underline{F}_{s,y}(x) = \delta(x)$ yields a Green's function $\underline{G}(k_x, y)$. For a specified diplacement of the infinitely thin beam at $y = 0$, $\underline{u}_y(x,0)|_{x=-B/2..B/2} = U_{y,0}$, the integral equation

$$\underline{u}_y(x,0) = \int_{-B/2}^{B/2}\mathcal{F}^{-1}\{\underline{G}(k_x,0)\}|_{x-x'}\underline{F}_{s,y}(x',0)dx' \quad (8)$$

has to be solved to obtain the force distribution $\underline{F}_{s,y}(x,0)$ on the beam. The resulting resistance force F_{res} on the beam per unit length is determined by

$$F_{res} = \int_{-B/2}^{B/2}\underline{F}_{s,y}(x,0)\}dx, \quad (9)$$

and consequently $m_f = -\Re\{F_{res}\}/\omega^2$ and $\alpha = \Im\{F_{res}\}/\omega$.

We solve this integral equation numerically by using the method of moments with rectangular basis functions and δ–weighting functions, where the area is discretized to $N = 2^n$ elements to take advantage of the FFT–algorithm (see, e. g. [12]).

NUMERICAL RESULTS

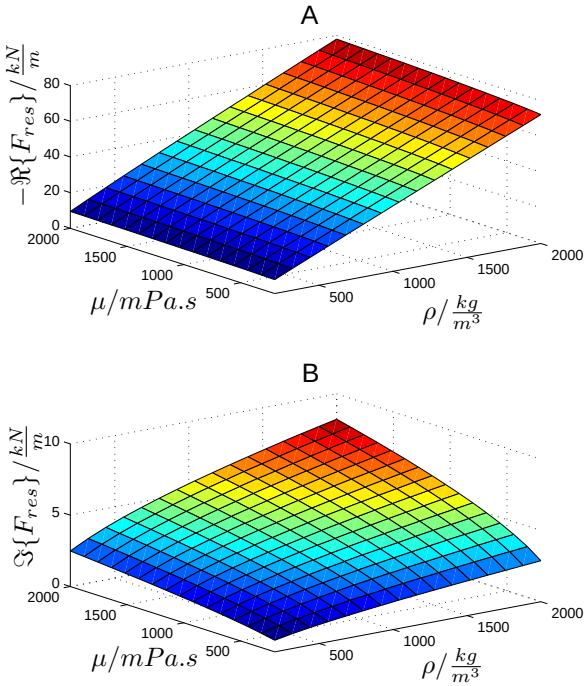

Figure 1. Resistance force F_{res} due to the added mass term (A: negative real part) and due to the damping coefficient (B: imaginary part) depending on the fluid properties ρ and μ on a thin beam of the width $W = 40\mu m$ vibrating at a frequency of $10kHz$

Fig. 1 shows the calculated resistance on an infinitely long and thin beam of the width $W = 40\mu m$ depending on the fluid parameters. While the resistance on a vibrating cylinder (Eqn. 4) depends on the ratio of μ/ρ only, the resistance on the vibrating thin beam depends on variations of μ and ρ seperately. Compared to the resistance due to viscous damping, the resistance due to added mass shows a stronger dependance on the density. This allows both, density and viscosity sensing with a single device.

ELECTRICAL MODEL

In the vicinity of a resonant mode, the added mass term m_f as well as the damping coefficient α in Eqn. 2 are almost constant, so the vibrating beam structure can be approximately represented by a single lumped, damped spring–mass oscillator for each mode. The governing differential equation is

$$m_n \cdot \ddot{x} + d_n \cdot \dot{x} + k_n \cdot x = f(t) \quad (10)$$

where $m_n = L_b(\rho_b A + m_f)$ (cf. Eqn. 3) is the total equivalent mass of mode n, $d_n = L_b\alpha$ is the respective damping coefficient, $k_n = L_b(EJ\kappa_n^4 + N\kappa_n^2)$ is the

equivalent spring constant, and x is a generalized displacement coordinate. The driving Lorentz force is generated according to $\vec{F}_L(t) = i_1(t) \cdot (\vec{l} \times \vec{B})$, where $i_1(t)$ is the time–varying current in the conductor of length $|\vec{l}|$. A permanent magnet is used to generate the external magnetic field $\vec{B}$. The driving term in Eqn. 10 is the total force, $f(t) = |\vec{F_L}|$ acting on the beam. For the mechanical oscillator, an equivalent electrical parallel resonance circuit can be derived since it is characterized by the same differential equation:

$$C_n \cdot \ddot{y} + G_n \cdot \dot{y} + L_n \cdot y = i_2(t) \tag{11}$$

where C_n, G_n, and L_n are the parameter values of the parallel resonance circuit shown in Fig. 2, representing m_n, d_n, and k_n of the mechanical oscillator respectively, and $i_2(t)$ is the driving current representing the Lorentz force $f(t)$. An immersion of the beam in the liquid under investigation yields an additional damping and a shift in the resonance frequency, which is modeled by an additional parallel resistance R_L and an additional capacitance C_L in the equivalent circuit. The electro–mechanical coupling factor results from

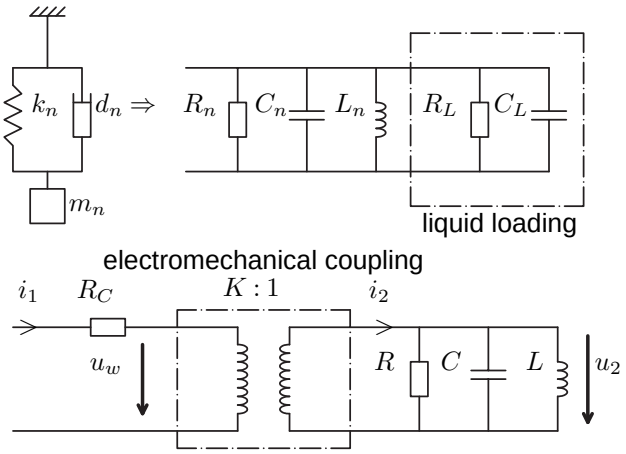

Figure 2. Equivalent electrical circuit of the coupled system.

the Lorentz force on the conductive path:

$$K = \frac{i_2}{i_1} \propto B \cdot L_b \cdot, \tag{12}$$

where B is the strength of the permanent magnetic field. In the equivalent circuit, the voltage u_2 corresponds to the generalized velocity $\dot{x}$ and thus the displacement is proportional to the current i_L through the inductance, i. e. $x_n \propto i_L$. The equivalent circuit model of the coupled system is depicted in Fig. 2, where the conductive path is represented by the resistance R_C, neglecting its inductance and the capacitance between electrodes. The measurable impedance on the primary side is thus given by

$$Z(\omega) = R_C + \underbrace{K^2 \cdot \frac{1}{\frac{1}{R} + j\omega C + \frac{1}{j\omega L}}}_{\Delta Z(\omega)} . \tag{13}$$

To identify the basic resonant modes and the associated resonance frequencies of the beam, a 3D simulation of the mechanical structure without liquid loading using the finite element method (FEM) was carried out. The simulation results depicted in Fig. 3 show three (unsymmetrical) normal modes (N1, N3, N5), two torsional modes (T1 and T3), and the fundamental shear mode (S1). The orientation of the external magnetic field determines which modes are excited preferably (see arrows in Fig. 3). Each mode is characterized by different electrical parameters C_n, G_n, and L_n in the electrical equivalent circuit.

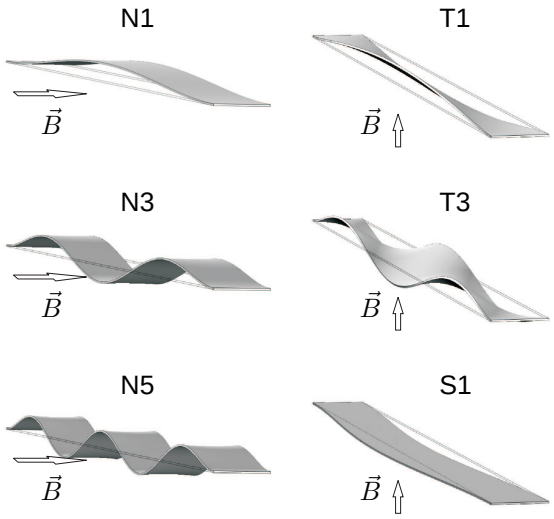

Figure 3. The eigenmodes of the beam structure. The arrows indicate the orientation of the magnetic field used to excite the respective modes.

FABRICATION

To fabricate the micromachined sensor chip shown in Fig. 4, a 350 μm thick (100) silicon wafer has been coated with silicon nitride (Si_3N_4) on both sides featuring a thickness of 320 nm. Next, a Ti–Au–Cr layer with a thickness of 50–100–30 nm has been deposited and structured to create the connection leads and the bond pads. A low stress silicon nitride (SiN_x) protective film of 1000 nm has been applied using a low temperature PECVD process. After creating the apertures for the bonding pads and the backside etch windows by means of reactive ion etching, thin membranes have been manufactured using a KOH based anisotropic backside wet etching process. In order to obtain the required bridges, the membranes have then been structured from the frontside using a reactive ion etching process. Finally, the chromium has been removed from the bond pads by means of wet–etching. Both silicon nitride layers form the bridge featuring a total thickness of 1.3 μm.

MEASUREMENTS

At the resonance frequencies, the displacement amplitude reaches a local maximum. In general, an optical readout is well suited to detect the resonant behaviour of cantilevers [13]. However, in order to reduce the number of external devices and to eliminate the

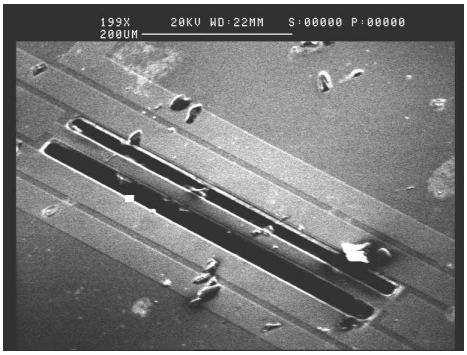

Figure 4. SEM micrograph of the beam structure. The bridge carries the conductive excitation path. The length is $L_b = 720\ \mu m$, cross–sectional dimensions are $40 \times 1.3\ \mu m$. The particles are considered to be process artefacts.

need for calibration procedures, an electronic readout circuit is preferred. A common successful approach is based on the piezoresistive effect [14]. In the current setup, the change in the resistance of the metallic conductor was estimated to be in the range of milliohms. The piezoresistive effect could be increased by using semiconductor materials for sensing mechanical strain [15]. This piezoresistive response is not covered by our equivalent circuit, which considers only inductive effects, which can be measured by means of impedance spectroscopy. In our case of an electromagnetically driven beam, the change in the impedance $\Delta Z(\omega)$ at resonance is small but measurable with an Agilent 4294A impedance analyzer.

Thus, measurements of the impedance spectrogram were carried out to identify the resonant modes in air. In Fig. 5 the impedance spectra for the two orthogonal arrangements of the magnetic field are shown. It can be seen, that for each arrangement different dominant modes appear, which can be associated with dominant normal or torsional modes. The shear mode (S1), however could not be detected this way.

SUMMARY AND OUTLOOK

In this contribution a model of a vibrating doubly clamped beam was presented which allows to simulate the effect of a liquid load. An electrical equivalent model was presented which allows to estimate the effect on the measurable change in impedance at the resonance frequencies. This allows a readout of the relative vibrational amplitude by means of impedance spectroscopy.

Due to the variety of vibrational modes offered, the doubly clamped beam structure is particularly suited as a viscosity and density sensor.

Further improvements in the readout are necessary to use the device as a sensor. For instance increasing the length of the conductive path used for the electro–mechanical coupling will result in a quadratic increase of the sensor signal when pursuing the inductive readout. Accurate measurements of the frequency response will allow an extraction of the parameters of the electrical model and consecutively the calculation of the forces caused by the liquid loading. The fluid model then allows a determination of the mass density

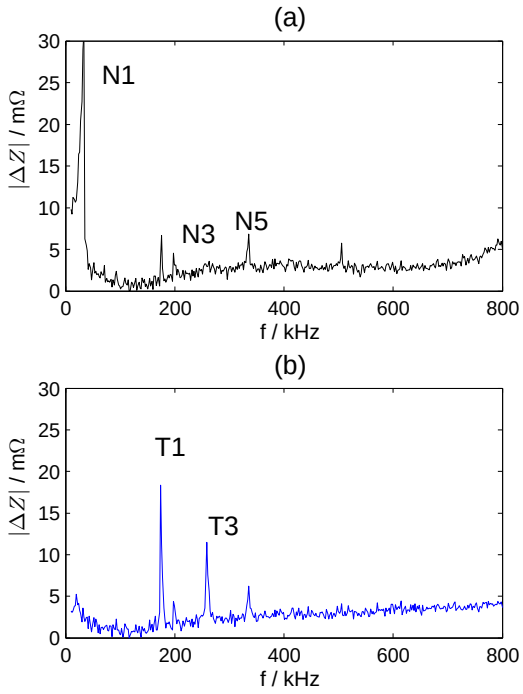

Figure 5. Measured impedance spectra of the sensor in air using both the (a) normal excitation (left in Fig. 3) and the (b) shear excitation (right in Fig. 3).

and viscosity of the liquid under investigation.

ACKNOWLEDGEMENTS

We would like to thank Wolfgang Hilber for the SEM analysis of the micromachined structure.

REFERENCES

[1] J. E. Sader, *Journal of Applied Physics*, Vol. 84 Nr. 1, 1998
[2] M. Villarroya et al, *Research in Microelectronics and Electronics*, p. 197–200 vol.1, 2005
[3] C. Vancura et al, *Transducers'05*, p. 640–643, Seoul, 2005
[4] L. F. Matsiev, *1999 IEEE Ultrasonics Symposium*, p. 457–460, 1999
[5] S. J. Martin et al, *Sensors and Actuators A 44*, Elsevier, p. 209–218, 1994
[6] B. Jakoby et al, *Sensors and Actuators A 123–124*, Elsevier, p. 274–280, 2005
[7] A. Agoston et al, *Sensors and Actuators A 123–125*, Elsevier, p. 82–86, 2005
[8] O. Brand et al, *Transducers'97*, p. 121–124, 1997
[9] R. Beigelbeck and B. Jakoby, *Journal of Applied Physics*, 95 (9), P. 4989-4996, 2004
[10] F. Ziegler, *Technische Mechanik der festen und der flüssigen Körper*, 3^{rd} ed., Springer, 1998
[11] E. O. Tuck, *Journal of Engineering Math*, Vol. 3 (1969) 29-44
[12] B. Jakoby et al, *IEEE Transactions on Ultrasonics, Ferroelectrics and Frequency Control, Vol. 47*, p.651-656, 2000
[13] F. Keplinger et al, *Sensors and Actuators A 110*, p. 112–118, Elsevier, 2004
[14] S. Daisuke et al, *Sensors and Actuators A 123–124*, Elsevier, 2005
[15] G. T. A. Kovacs, *Micromachined Transducers Sourcebook*, McGraw–Hill, 1998